

observed pairwise F_{ST} between European populations in the 1000 Genomes project, which was 0.013 ± 0.00059 between Finnish and Italian individuals (Fig. 3B). These estimates suggest greater genetic stratification among Stone Age European groups as compared with current-day groups of European ancestry (7) but that this stratification in Stone Age Europe was correlated with the mode of subsistence instead of geography, as in current-day Europe (23).

The distinct features of the two Neolithic Scandinavian groups—nonsymmetric gene-flow into farmers, low level of diversity among hunter-gatherers, and strong differentiation between groups—have important implications for our understanding of the demographic histories of these groups. The greater diversity in the farmer population may have been influenced by gene flow from hunter-gatherers. However, the low level of genetic diversity in Neolithic hunter-gatherers likely has a demographic explanation, similar to that of the Iberian Mesolithic individual (8). Although we cannot exclude that this low diversity is a feature restricted to the Gotland island hunter-gatherer population, the low diversity may be due to the fact that hunter-gatherer ancestors resided in ice-free refugia in Europe during the Last Glacial Maximum (LGM), potentially causing population bottlenecks. Climatic changes and occasional population crashes also likely affected the population sizes of hunter-gatherers (24, 25). Furthermore, mobility may have decreased among late hunter-gatherer groups, especially when settling in coastal areas (20). Meanwhile, the population ancestral to the Neolithic farmers, that later were to expand across Europe, resided in warmer areas that could sustain larger population sizes during the LGM. Although it is possible that climate also affected populations in southern Eurasia, it may have been in a different manner (26), and farming economies are associated with greater carrying capacity than those of hunter-gatherer economies. It is likely that several factors contributed to the different levels of genetic diversity, and disentangling these processes and assessing their generality in prehistoric Europe may be possible as more genomic data from a wider geographic and temporal range becomes available.

References and Notes

- V. G. Childe, *The Dawn of European Civilization* (Kegan Paul, London, 1925).
- P. Menozzi, A. Piazza, L. Cavalli-Sforza, *Science* **201**, 786–792 (1978).
- M. P. Malmer, *The Neolithic of South Sweden: TRB, GRK, and STR*. (Almqvist & Wiksell International, Stockholm, 2002).
- B. Bramanti *et al.*, *Science* **326**, 137–140 (2009).
- H. Malmström *et al.*, *Curr. Biol.* **19**, 1758–1762 (2009).
- G. Brandt *et al.*, *Science* **342**, 257–261 (2013).
- P. Skoglund *et al.*, *Science* **336**, 466–469 (2012).
- I. Olalde *et al.*, *Nature* **507**, 225–228 (2014).
- A. Keller *et al.*, *Nat. Commun.* **3**, 698 (2012).
- Q. Fu *et al.*, *Curr. Biol.* **23**, 553–559 (2013).
- A. O. Karlsson, T. Wallerström, A. Götherström, G. Holmlund, *Eur. J. Hum. Genet.* **14**, 963–970 (2006).
- C. Basu Mallick *et al.*, *PLOS Genet.* **9**, e1003912 (2013).
- M. Raghavan *et al.*, *Nature* **505**, 87–91 (2014).
- K. Tambets *et al.*, *Am. J. Hum. Genet.* **74**, 661–682 (2004).
- N. Patterson *et al.*, *Genetics* **192**, 1065–1093 (2012).
- P. Skoglund *et al.*, *Proc. Natl. Acad. Sci. U.S.A.* **111**, 2229–2234 (2014).
- Materials and methods are available as supplementary materials on Science Online.
- I. Lazaridis *et al.*, <http://arxiv.org/abs/1312.6639> (2013).
- L. Klassen, in *The Neolithisation of Denmark: 150 Years of Debate*, A. Fischer, K. Kristiansen, Eds. (J. R. Collis, Sheffield, UK, 2002), pp. 305–317.
- G. Bailey, in *Mesolithic Europe*, G. Bailey, P. Spikings, Eds. (Cambridge Univ. Press, Singapore, 2008), chap. 14.
- M. Meyer *et al.*, *Science* **338**, 222–226 (2012).
- G. R. Abecasis *et al.*, *Nature* **491**, 56–65 (2012).
- J. Novembre *et al.*, *Nature* **456**, 98–101 (2008).
- F. Riede, *Hum. Biol.* **81**, 309–337 (2009).
- S. Shennan, K. Edinborough, *J. Archaeol. Sci.* **34**, 1339–1345 (2007).
- B. Weninger *et al.*, *Quat. Res.* **66**, 401–420 (2006).
- Acknowledgments:** We thank L. Gattepaille, M. Metspalu, T. Naidoo, M. Rasmussen, S. Rasmussen, D. Reich, E. Salmela, and P. Wallin for technical assistance and discussions. The SNP data for the modern-day Swedish individuals is available from P. Hall at the Karolinska Institute under a materials transfer agreement. We thank the late L. Beckman for contributing the Saami samples; K.T. (ktambets@gmail.com) retains governance over the Saami and the Mari samples. This project was supported by grants from the Nilsson-Ehle Foundation (P.S.), Helge Ax:son Foundation (P.S.), Royal Swedish Academy of Science (FOA12H-177 to P.S.), Danish National Research Foundation (E.W. and M.R.), Swedish Research Council (J.A. and J.S.), Berit Wallenberg Foundation (J.A. and J.S.), Wenner-Gren Foundations (T.G.) and European Research Council (M.J.). P.S., H.M., A.G., and M.J. conceived and designed the study. E.W., J.S., A.G., and M.J. supervised the study. H.M., A.O., M.R., and C.V. generated DNA sequence data from ancient human remains. P.S. processed and prepared the data. P.S., H.M., and T.G. analyzed the genetic data, supervised by M.J. with the following contributions: mtDNA and Y-chromosome (H.M. and P.S.); functional SNPs (T.G. and P.S.); and contamination, biological sex, and population genetic analyses (P.S.). K.-G.S., J.S., and J.A. provided archaeological information and interpretation. P.H., K.T., and J.P. contributed samples. P.S., H.M., J.S., A.G., and M.J. wrote the manuscript with input from all authors. Data are available from the European Nucleotide Archive under accession no. PRJEB6090, and data aligned to the human reference genome are available at www.ebc.uu.se/Jakobsson. The authors declare no competing interests.
- Supplementary Materials**
www.sciencemag.org/content/344/6185/747/suppl/DC1
Materials and Methods
Supplementary References
Figs. S1 to S9
Tables S1 to S16
References (27–101)
17 March 2014; accepted 16 April 2014
Published online 24 April 2014;
10.1126/science.1253448

Late Pleistocene Human Skeleton and mtDNA Link Paleoamericans and Modern Native Americans

James C. Chatters,^{1*} Douglas J. Kennett,² Yemane Asmerom,³ Brian M. Kemp,⁴ Victor Polyak,³ Alberto Nava Blank,⁵ Patricia A. Beddows,⁶ Eduard Reinhardt,⁷ Joaquin Arroyo-Cabrales,⁸ Deborah A. Bolnick,⁹ Ripan S. Malhi,¹⁰ Brendan J. Culleton,² Pilar Luna Erreguerena,¹¹ Dominique Rissolo,¹² Shanti Morell-Hart,¹³ Thomas W. Stafford Jr.¹⁴

Because of differences in craniofacial morphology and dentition between the earliest American skeletons and modern Native Americans, separate origins have been postulated for them, despite genetic evidence to the contrary. We describe a near-complete human skeleton with an intact cranium and preserved DNA found with extinct fauna in a submerged cave on Mexico's Yucatan Peninsula. This skeleton dates to between 13,000 and 12,000 calendar years ago and has Paleoamerican craniofacial characteristics and a Beringian-derived mitochondrial DNA (mtDNA) haplogroup (D1). Thus, the differences between Paleoamericans and Native Americans probably resulted from in situ evolution rather than separate ancestry.

Genetic studies of contemporary Native Americans and late prehistoric skeletal remains from the Americas have consistently supported the idea that Native Americans are descended from Siberian ancestors who moved into eastern Beringia between 26,000 and 18,000 years ago (26 to 18 ka), spreading southward into the Americas after 17 ka (1). A complete genome analysis of the 12.6-ka Anzick infant from Montana (2), and mitochondrial DNA (mtDNA) from the 14.1-ka coprolites from Paisley Caves in Oregon (3) and mtDNA from other early (10.5 to 10.2 ka) remains from Nevada and Alaska (4, 5) support this hypothesis. With Anzick linked to the Clovis culture and Paisley Caves to the West-

ern Stemmed tradition—North America's two widespread early archaeological complexes—the genetic evidence for a Beringian origin of the earliest inhabitants of western North America is compelling.

The ancestry of the earliest Americans is still debated, however, because the oldest skeletal remains from the Americas (>9 ka, the Paleoamericans) consistently fail to group morphometrically with modern Native Americans, Siberians, and other northeast Asians (6). Paleoamericans exhibit longer, narrower crania and smaller, shorter, more projecting faces than later Native Americans (7). In nearly all cases, they are morphologically most similar to modern peoples of Africa,

Australia, and the southern Pacific Rim (7–9). Polymorphic dental traits currently found in East Asia also distinguish later Native Americans (10),

¹Applied Paleoscience and DirectAMS, 10322 NE 190th Street, Bothell, WA 98011, USA. ²Department of Anthropology and Institutes of Energy and the Environment, Pennsylvania State University, University Park, PA 16802, USA. ³Department of Earth and Planetary Sciences, University of New Mexico, Albuquerque, NM 87131-0001, USA. ⁴Department of Anthropology and School of Biological Sciences, Washington State University, Pullman, WA 99164, USA. ⁵Bay Area Underwater Explorers, Berkeley, CA, USA. ⁶Department of Earth and Planetary Sciences, Northwestern University, Evanston, IL 60208, USA. ⁷School of Geography and Earth Sciences, McMaster University, Hamilton, Ontario L8S 4K1, Canada. ⁸Instituto Nacional de Antropología e Historia, Colonia Centro Histórico, 06060, Mexico City, DF, Mexico. ⁹Department of Anthropology and Population Research Center, University of Texas at Austin, Austin, TX 78712, USA. ¹⁰Institute for Genomic Biology, University of Illinois, Urbana-Champaign, IL 61801, USA. ¹¹Subdirección de Arqueología Subacuática, Instituto Nacional de Antropología e Historia, 06070 Mexico City, Mexico. ¹²Waitt Institute, La Jolla, CA 92038-1948, USA. ¹³Department of Anthropology, Stanford University, Stanford, CA 94305, USA. ¹⁴Centre for AMS ¹⁴C, Department of Physics and Astronomy, Aarhus University, Aarhus, Denmark, and Centre for GeoGenetics, Natural History Museum of Denmark, Geological Museum, Copenhagen, Denmark.

*Corresponding author. E-mail: paleosci@gmail.com

who tend to exhibit such specialized (Sinodont) traits as winged, shovel-shaped upper incisors, three-rooted lower first molars, and small or absent third molars; from Paleoamericans, who exhibit a less specialized (Sundadont) morphology (7). These differences suggest that America was colonized by separate migration events from different parts of Eurasia (11) or by multiple colonization events from Beringia (12), or that evolutionary changes occurred in the Americas after colonization (13).

To date, most genetic data are from immature individuals, such as the Anzick infant (2); fragmentary material, such as the remains from On Your Knees Cave (5); or human byproducts, such as the Paisley Cave coprolites (3). The one complete skull associated with ancient DNA (aDNA), Wizard's Beach (4), is a single early Holocene individual that groups morphometrically with modern Native Americans (9). Furthermore, genetic evidence from the earliest Americans—those predating 10 ka—is limited to northwestern North America (Fig. 1 and Table 1), leaving open the possibility of different geographic origins for Paleoamericans elsewhere in the hemisphere.

Resolution of this issue has also been hindered by the rarity of Paleoamerican skeletons. Remains

of no more than 30 individuals from North America, most of them fragmentary, predate 10 ka, and only 12 are directly dated (table S1). Furthermore, just 20 skeletons in this age range are reported for South America (14). Only five individuals, all from North America, securely predate 12 ka (Table 1). Of these five, only two have intact skulls and none possesses a complete dental assemblage.

Here we report a nearly complete, Late Pleistocene-age human skeleton (HN5/48) with intact dentition from Hoyo Negro (HN), a submerged collapse chamber in the Sac Actun cave system, eastern Yucatan Peninsula, Mexico (Fig. 1). HN lies at the confluence of three horizontal passages formed within a Cenozoic limestone platform (fig. S1). This and other cave systems in the Yucatan were accessible via sinkholes for much of the last glacial period, serving as natural traps for people and animals. They became inundated between 10 and 4 ka (15), as the glaciers melted. Sea-level change was predominantly eustatic in this tectonically stable region (16), with a moderate offset imposed by a global glacial isostatic adjustment (17). The remains of Pleistocene megafauna and pre-Maya humans occur in other cave systems, including eight partial human skeletons

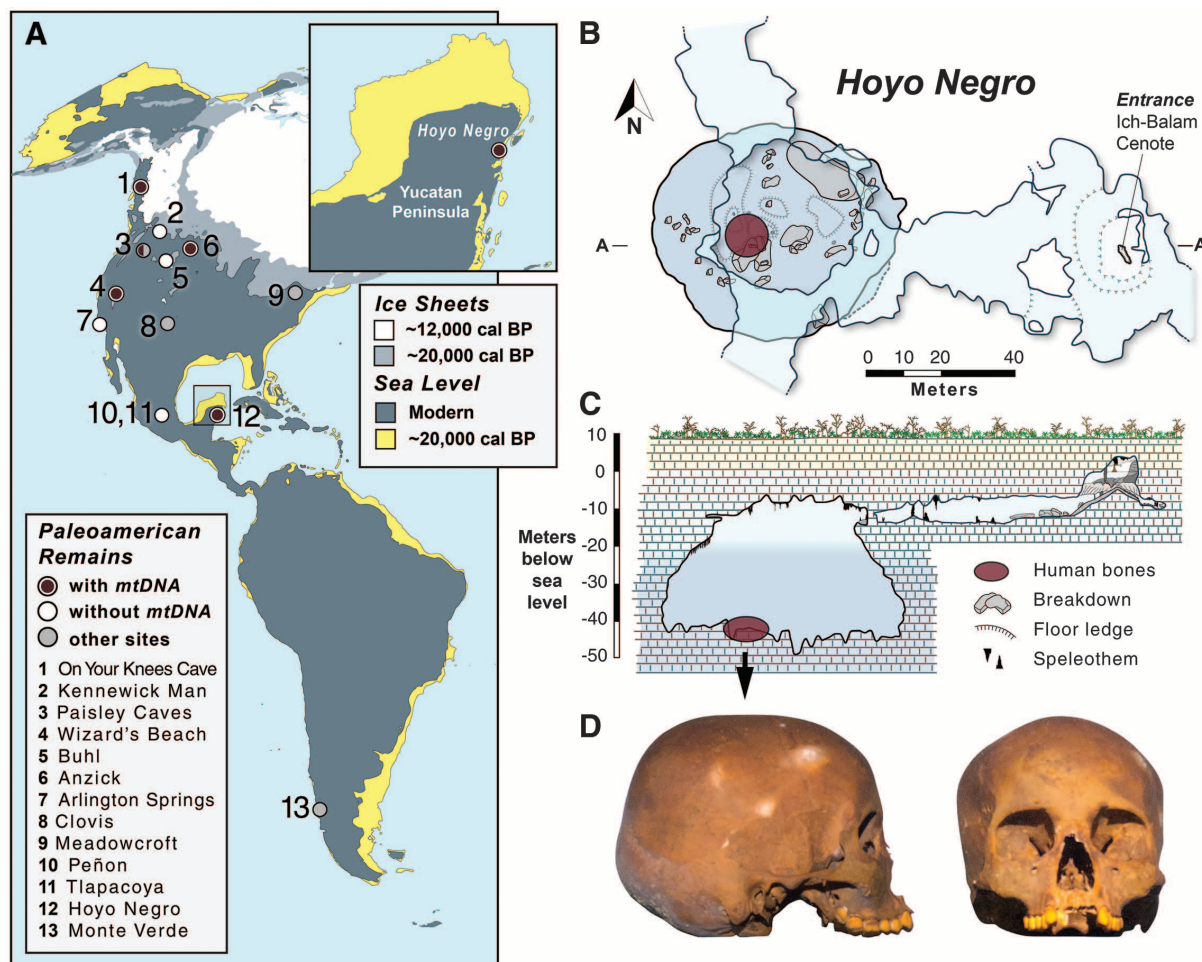


Fig. 1. The site and skull form of the HN human remains. HN5/48 was found far to the southeast of other ancient American skeletons from which DNA has been obtained (A). HN5/48 lies at the bottom of HN, a submerged

chamber shown in plan and profile (B and C). Paleoamerican features are visible in this view of the cranium (D). Paisley Cave is an early site with DNA but without Paleoamerican skeletal remains.

Table 1. Paleoamerican skeletons directly dated to >12 ka*† and all >10 ka skeletons from which aDNA has been extracted.

Skeleton	Location	¹⁴ C age	Age (calendar yr B.P.)	Skeletal assemblage	aDNA	aDNA reference
On Your Knees Cave	AK, USA	9200 ^{‡§}	~10,500–10,250	Mandible, carnivore-damaged skeletal fragments	mtDNA: D4h3a; Y: Q1a3a1a	(5)
Wizard’s Beach	NV, USA	9225 ± 60	10,560–10,250	Skull with partial dentition, partial skeleton	mtDNA: C1	(4)
Tlapacoya I	Mexico, EUM	10,200 ± 65	12,150–11,610	Calotte	No	—
Buhl	ID, USA	10,675 ± 95	12,740–12,420	Skull with partial dentition, partial skeleton (reburied)	No	—
Anzick 1	MT, USA	10,680 ± 50 [‡]	12,707–12,556	Neurocranium, four bones of infant	mtDNA: D4H3a Y: Q-L54(xM3)	(2)
Peñon III	Mexico, EUM	10,755 ± 75	12,770–12,560	Skull with partial dentition, partial skeleton	No	—
Arlington Springs	CA, USA	10,960 ± 80	13,010–12,710	Partial femora	No	—
HN	Quintana Roo, EUM	10,976 ± 20 [‡]	12,910–11,750	Skull with complete dentition, largely complete skeleton	mtDNA: D1	This article

*Claims of >13 ka for Naharon (Mexico) and Lapa Vermelha IV (Brazil) are not supported by evidence (table S1 footnotes). †For references, see table S1. ‡Mean of multiple measurements. §No standard deviation provided. ||Age range constrained by ¹⁴C and U-Th dates. Calibrations were computed in OXCAL 4.2, based on Reimer *et al.* (25).

found 20 km south of HN in the Tulum region. These individuals are inferred to predate 10 ka on the basis of their depth below sea level, but reliable radiometric dates on the skeletons are lacking.

HN is a 62-m-diameter, subterranean, bell-shaped, collapsed dissolution chamber (pit) containing the skeletons of one human and at least 26 large mammals (Fig. 1 and table S2). The three passages joining HN are 10 m below sea level (mbsl); the pit drops to a maximal depth of 55 mbsl. The bottom is strewn with roof-collapse boulders and marked by guano, accumulations of calcite raft sediment, and a few stalagmites. HN contains layered fresh and saltwater, with a halocline at 15 to 22 mbsl. This permeable aquifer tracks sea level to within 1 to 2 m. The skeletal material lies at the base of the pit, 600 m from the nearest entrance when it was a dry cave. HN is now accessible only by technical dive teams. Information collected to date has been derived primarily through videography, photography, minimal sampling, and three-dimensional modeling from remote images.

The faunal assemblage in the bottom of HN is composed of extinct taxa, including sabertooth (*Smilodon fatalis*), gomphothere (*Cuvieronius* cf. *tropicus*, a proboscidean), Shasta ground sloth (*Nothrotheriops shastensis*), and an unnamed megalonychid ground sloth, along with extant species, including puma, bobcat, coyote, Baird’s tapir, collared peccary, white-nosed coati, and a bear of the genus *Tremarctos* (table S2 and fig. S2). Animal bones are concentrated on the south side of the floor on wall projections or sloping boulders between 40 and 43 mbsl (28 to 31 m below the pit rim; figs. S3 and S4). The distribution and condition of elements are probably explained by the decomposition of the carcasses in water, which scattered bones toward the walls of the room during episodic flooding of the chamber (fig. S4).

Subaerial conditions existed in this room above 42 mbsl before inundation or recurred after short-lived episodes of water table rise, because some

bones of the human and one gomphothere are covered with patches of calcite speleothems in the form of 0.5 to 5-cm bushy crystals referred to here as florets. Florets develop from dripping water in a manner similar to stalagmites, growing from the mist/aerosol created by drip water hitting the cave floor.

Directly dating HN5/48 and the associated faunal assemblage is challenging because the conditions do not favor bone collagen preservation. Attempts to extract collagen from bone and tooth specimens for accelerator mass spectrometry (AMS) radiocarbon (¹⁴C) dating were unsuccessful. Multiple lines of evidence, however, indicate that the human remains and much of the faunal assemblage date to the latest Pleistocene. HN5/48 is associated by position and depth with the remains of multiple species of megafauna (sabertooth, gomphothere, and ground sloths) that were largely extinct in North America by 13 ka (18, 19). HN, therefore, trapped the animals before flooding. The age of the human skeleton is thus constrained by sea-level history after the Last Glacial Maximum (LGM) (17). Identifying the florets as subaerial deposits is consistent with the inundation of HN5/48 after 10 to 9.5 ka on the basis of global sea-level reconstructions (20, 21) and our independent evidence of cave flooding.

In 2013, our dive team collected florets formed on the surfaces of human bones (Fig. 2) for absolute age determinations with the uranium-thorium (U-Th) method. Nine U-Th dates on florets removed directly from the upper surfaces of these bones range from 12.0 ± 0.2 to 9.6 ± 0.1 ka (tables S3 and S4). This establishes a minimum age of ~12 ± 0.2 ka for the human skeleton. Independent AMS ¹⁴C measurements on enamel bioapatite from an upper third molar yielded statistically identical ¹⁴C ages of 10,970 ± 25 [Stafford Research sample no. 8205, University of California-Irvine AMS (UCIAMS) sample no. 119438] and 10,985 ± 30 years before the present (¹⁴C yr B.P.)

(Pennsylvania State University sample no. 5493, UCIAMS sample no. 123541), suggesting a calibrated age for the skeleton of ~12.9 to 12.7 ka. Bioapatite is subject to contamination by dissolved inorganic carbon (DIC) in groundwater, however. A 16,160 ± 78 ¹⁴C yr B.P. date on bioapatite from a rib of HN5/48 indicates that the rib was contaminated by fossil carbon, which may also have affected the enamel age. The 13-ka date must therefore be considered a maximum age for the skeleton. Furthermore, there could be a small reservoir effect if this individual consumed marine foods, but that appears unlikely because of light dental wear, severe dental caries, and paleoecological evidence for a terrestrial emphasis in the diet of the earliest Central Americans. Thus, we argue that this individual entered the cave system between 13.0 and 12.0 ka.

To determine whether the human bones and the associated gomphothere (fig. S5) are the same age, we obtained U-Th ages of florets from the larger animal’s pelvis and femur and ¹⁴C dates on its tooth enamel (table S3). Five U-Th dates range between 18.8 ± 0.3 and 11.9 ± 0.3 ka and indicate that the gomphothere was deposited by at least ~19 ka. Two AMS ¹⁴C dates on its tooth enamel suggest an age as early as 41.6 to 36.4 ka, but these teeth are heavily mineralized, and we cannot rule out DIC affecting this age estimate. Regardless, the U-Th and AMS ¹⁴C data are consistent with the hypothesis that HN trapped animals during the latest Pleistocene, when the upper horizontal passages were accessible, with western Caribbean sea level below 10 mbsl. The U-Th dates also indicate that HN was largely subaerial and primarily dry above 42 mbsl between 19.0 and 9.5 ka.

⁸⁷Sr/⁸⁶Sr and δ²³⁴U values demonstrate that the florets precipitated under relatively stable vadose, subaerial conditions throughout this interval (tables S4 and S5). Floret formation below 42 mbsl terminated at 9.6 ± 0.1 ka, consistent with the hypothesis that inundation of the cave

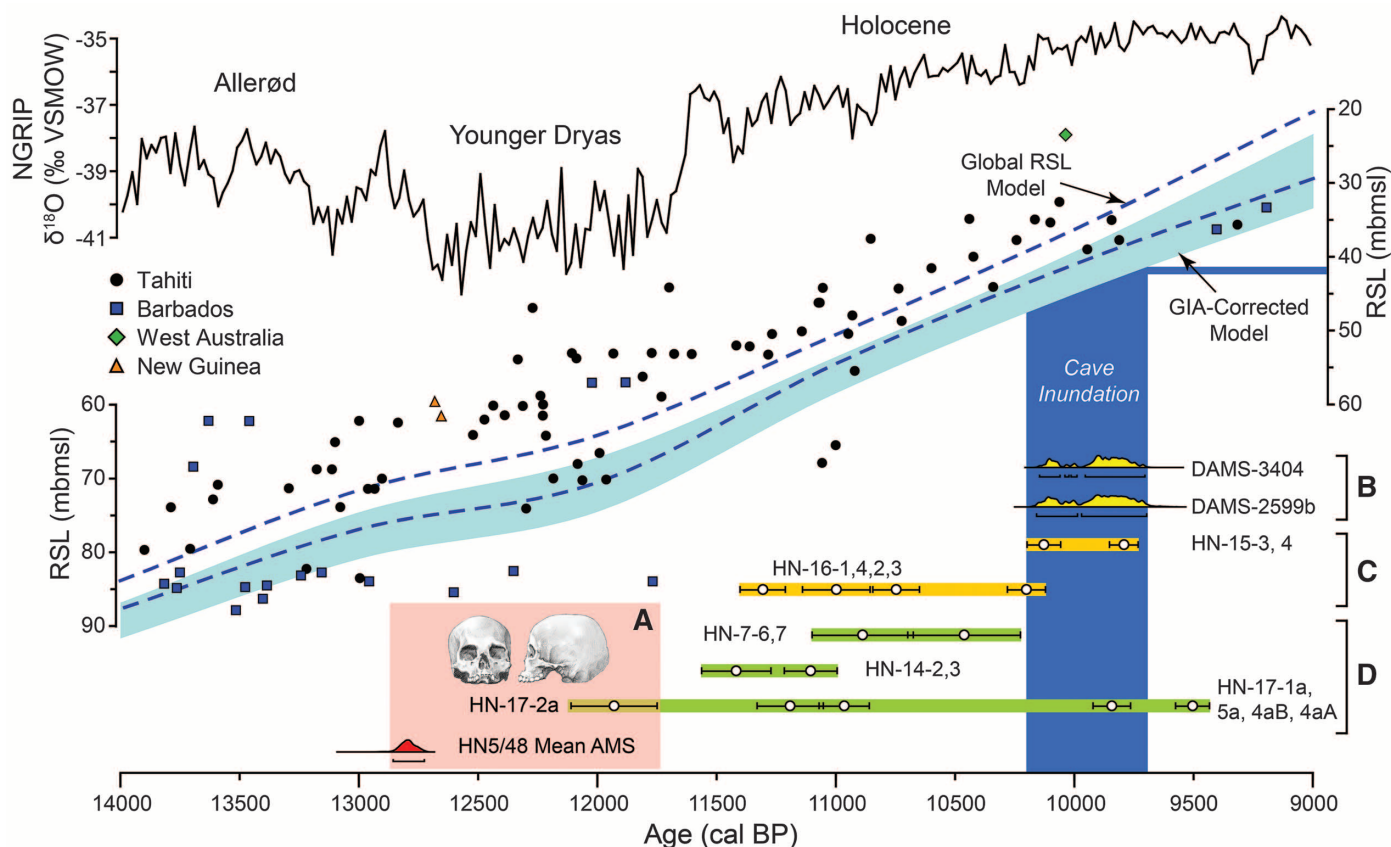


Fig. 2. Radiocarbon and U-Th dates from HN compared to relative sea level (RSL). Radiocarbon dates on a human tooth (red histogram) and U-Th dates from calcite florets on human bones [green bars in (D)] place HN5/48 between 12,910 and 11,750 calendar yr B.P. [pink bar in (A)]. Calcite florets (C and D) and guano deposits [yellow histograms in (B)] ceased forming when

rising sea level surpassed 42 mbsl and permanently inundated the human remains (blue bar). The global RSL model presented is from corals with a $^{234}\text{U}/^{238}\text{U}$ activity range of 1.137 to 1.157 (21), modified by an estimated glacial isostasy adjustment (GIA) of 3.5 m (20). Measurement standards: NGRIP, North Greenland Ice Core Project; VSMOW, Vienna standard mean ocean water.

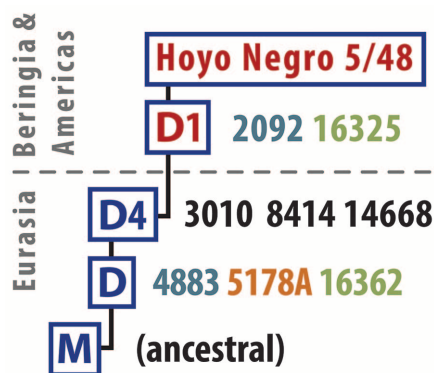


Fig. 3. Base-pair substitutions (numbers) confirming the presence of mtDNA haplogroups D and D1 in HN5/48. Colors represent substitutions confirmed in multiple extracts with restriction fragment length polymorphism and DNA sequencing (orange), multiple extracts with DNA sequencing (green), and a single extract with DNA sequencing (blue).

between 10.2 and 9.5 ka, which is also consistent with these reconstructions (table S3). Thus, the age range for HN5/48 (13 to 12 ka) is supported by this larger geochronological framework.

HN5/48 is the largely complete, well-preserved skeleton of a gracile, small-statured (149 ± 4 cm) female estimated to have been 15 to 16 years old. All skeletal elements are intact, except for apparent perimortem fractures of pubic bones, trauma that is consistent with a fall into a shallow pool from one of the upper passages. Cranial and dental characteristics are comparable to those of other, less complete pre-10-ka Paleoamerican skeletons, including Peñon, Buhl, and Wilson-Leonard [(7, 8) table S1], and to those of Upper Paleolithic humans across Eurasia (22). Measurements from a three-dimensional digital model show the cranium to be long and high, with a pronounced forehead and projecting, sharply angled occipital (Fig. 1 and fig. S6). The upper face is short, broad, and small relative to the neurocranium, with low, wide-set eye orbits and a broad nose. It exhibits moderate alveolar prognathism and lacks the broad, everted zygomatics characteristic of late Holocene and contemporary Native Americans. The palate is long and parabolic, with moderately shoveled upper central incisors (a Sinodont

trait), a lack of double shoveling, no deflecting wrinkle on the lower first molar, third molars approximately equal in size to the second molars (Sundadont traits), and a strongly developed Carabelli's cusp on the upper first molar.

HN5/48 is among the small group of Paleoamerican skeletons, a group that is morphologically distinct from Native Americans. We extracted DNA from the skeleton's upper right third molar and analyzed the mtDNA using methods developed for poorly preserved skeletal elements, with independent replication. The mtDNA haplogroup for the HN skeletal remains was determined through restriction fragment analysis, direct Sanger sequencing, and second-generation sequencing after target enrichment. The Alu1 5176 site loss, in combination with Sanger and Illumina sequence data, confirm its placement in haplogroup D, subhaplogroup D1 (Fig. 3). Subhaplogroup D1 is derived from an Asian lineage but occurs only in the Americas, having probably developed in Beringia after divergence from other Asian populations (1).

D1 is one of the founding lineages in the Americas (1). Subhaplogroup D1 occurs in 10.5% of extant Native Americans (23), with a high frequency of 29% in indigenous people from Chile and Argentina (24). This suggests that HN5/48

occurred in parallel with rising sea levels (Fig. 2). AMS ^{14}C dates of seeds from nearby ostracod-bearing guano deposited in shallow water range

descended from the population that carried the D1 lineage to South America. The discovery of a member of subhaplogroup D1 in Central America, ~4000 km southeast of any other pre-10-ka DNA in the Americas, greatly extends the geographic distribution of Pleistocene-age Beringian mtDNA in the Western Hemisphere.

HN5/48 shows that the distinctive craniofacial morphology and generalized dentition of Paleoamericans can co-occur with a Beringian-derived mtDNA haplogroup. This 13- to 12-ka Paleoamerican skeleton thus suggests that Paleoamericans represent an early population expansion out of Beringia, not an earlier migration from elsewhere in Eurasia. This is consistent with hypotheses that both Paleoamericans and Native Americans derive from a single source population, whether or not all share a lineal relationship. In light of this finding, the differences in craniofacial form between Native Americans and their Paleoamerican predecessors are best explained as evolutionary changes that postdate the divergence of Beringians from their Siberian ancestors.

References and Notes

1. E. T. Tamm *et al.*, *PLOS ONE* **2**, e829 (2007).
2. M. Rasmussen *et al.*, *Nature* **506**, 225–229 (2014).
3. D. L. Jenkins *et al.*, *Science* **337**, 223–228 (2012).
4. F. A. Kaestle, D. G. Smith, *Am. J. Phys. Anthropol.* **115**, 1–12 (2001).
5. B. M. Kemp *et al.*, *Am. J. Phys. Anthropol.* **132**, 605–621 (2007).
6. J. A. Raff, D. A. Bolnick, *Nature* **506**, 162–163 (2014).
7. D. G. Steele, J. F. Powell, in *Who Were the First Americans?*, R. Bonnichsen, Ed. (Center for the Study of the First Americans, Oregon State University, Corvallis, OR, 1999), pp. 25–40.
8. R. González-José *et al.*, *Am. J. Phys. Anthropol.* **128**, 772–780 (2005).
9. J. F. Powell, W. A. Neves, *Am. J. Phys. Anthropol.* **110** (suppl. 29), 153–188 (1999).
10. C. G. Turner 2nd, *Am. J. Phys. Anthropol.* **82**, 295–317 (1990).
11. M. M. Lahr, *Evol. Anthropol.* **6**, 2–6 (1997).
12. J. C. Chatters, in *Human Variation in the Americas: The Integration of Archaeology and Biological Anthropology*, B. M. Auerbach, Ed. (Occasional Paper 38, Center for Archaeological Investigations, Southern Illinois Univ., Carbondale, IL, 2010), pp. 51–76.
13. J. F. Powell, *The First Americans: Race, Evolution, and the Origin of Native Americans* (Cambridge Univ. Press, Cambridge, 2004).
14. W. A. Neves *et al.*, in *Paleoamerican Odyssey*, K. E. Graff, C. V. Ketron, M. R. Waters, Eds. (Center for the Study of the First Americans, College Station, TX, 2013), pp. 397–412.
15. W. R. Peltier, R. G. Fairbanks, *Quat. Sci. Rev.* **25**, 3322–3337 (2006).
16. B. J. Szabo, W. C. Ward, A. E. Weidie, M. J. Brady, *Geology* **6**, 713–715 (1978).
17. G. A. Milne, M. Peros, *Global Planet. Change* **107**, 119–131 (2013).
18. R. W. Graham, in *The World of Elephants (La Terra degli Elefanti)—Proceedings of the 1st International Congress (Atti del 1° Congresso Internazionale)*, G. Cavarretta *et al.*, Eds. (Consiglio Nazionale delle Ricerche, Rome, 2001), pp. 707–709.
19. G. Haynes, *Quat. Int.* **285**, 89–98 (2013).
20. E. Bard, B. Hamelin, D. Delanghe-Sabatier, *Science* **327**, 1235–1237 (2010).
21. M. Medina-Elizalde, *Earth Planet. Sci. Lett.* **362**, 310–318 (2013).
22. M. M. Lahr, *Evolution of Modern Human Diversity* (Cambridge Univ. Press, Cambridge, 1996).
23. U. A. Perego *et al.*, *Genome Res.* **20**, 1174–1179 (2010).
24. M. de Saint Pierre *et al.*, *PLOS ONE* **7**, e43486 (2012).
25. P. J. Reimer *et al.*, *Radiocarbon* **55**, 1869–1887 (2013).

Acknowledgments: Data reported here are available in tables S2 to S5 and at GenBank (accession no. KJ710435). Support was provided by the National Geographic Society, the Archaeological Institute of America, the Waitt Institute, the Instituto Nacional de Antropología e Historia, NSF (Y.A., V.P., and D.K.), Pennsylvania State University, the University of New Mexico, the University of Texas at Austin, the University of Illinois, Urbana-Champaign, and DirectAMS.

Supplementary Materials

www.sciencemag.org/content/344/6185/750/suppl/DC1

Materials and Methods

Figs. S1 to S13

Tables S1 to S5

Additional Acknowledgments

References (26–107)

25 February 2014; accepted 18 April 2014

10.1126/science.1252619

Neurosensory Perception of Environmental Cues Modulates Sperm Motility Critical for Fertilization

Katherine McKnight,¹ Hieu D. Hoang,² Jeevan K. Prasain,³ Naoko Brown,⁴ Jack Vibbert,² Kyle A. Hollister,⁵ Ray Moore,³ Justin R. Ragains,⁵ Jeff Reese,^{4,6} Michael A. Miller^{2*}

Environmental exposures affect gamete function and fertility, but the mechanisms are poorly understood. Here, we show that pheromones sensed by ciliated neurons in the *Caenorhabditis elegans* nose alter the lipid microenvironment within the oviduct, thereby affecting sperm motility. In favorable environments, pheromone-responsive sensory neurons secrete a transforming growth factor- β ligand called DAF-7, which acts as a neuroendocrine factor that stimulates prostaglandin-endoperoxide synthase [cyclooxygenase (Cox)]-independent prostaglandin synthesis in the ovary. Oocytes secrete F-class prostaglandins that guide sperm toward them. These prostaglandins are also synthesized in Cox knockout mice, raising the possibility that similar mechanisms exist in other animals. Our data indicate that environmental cues perceived by the female nervous system affect sperm function.

Diet and environment have profound, yet largely unexplained effects on fertility in many animals (1, 2). Essential components of the mammalian diet include the polyunsaturated fatty acids (PUFAs), which are oxidized into labile signaling molecules called prostaglandins (fig. S1). The F-class prostaglandins are among the most abundant and ubiquitous members. Prostaglandins are critical for reproduction (3), but their functions and regulatory mechanisms are incompletely understood. For instance, in vitro studies have shown that prostaglandins induce Ca^{2+} influx into human sperm via the CatSper channel (4, 5).

The biological role of this mechanism is not clear, largely because monitoring sperm behavior in the female reproductive tract is difficult.

Cyclooxygenase (Cox) enzymes, the targets of nonsteroidal anti-inflammatory drugs, are thought to be the exclusive enzymatic initiators of prostaglandin synthesis (3). Prostaglandin species are also formed nonenzymatically under conditions of high oxidative stress (6). These latter prostaglandins, which are esterified to phospholipids, lack biological regulation and stereoselective generation. The nematode *Caenorhabditis elegans* generates specific F-class prostaglandins, including prostaglandin

F1 α (PGF1 α) and PGF2 α stereoisomers independent of Cox (7, 8) (fig. S1). Prostaglandin metabolism is regulated and has an important function in fertilization (8–10). Hence, *C. elegans* possesses an alternative metabolic pathway for F-class prostaglandin synthesis.

Oocytes synthesize numerous F-class prostaglandins from PUFA precursors provided in yolk lipoprotein complexes (8, 9). These prostaglandins function collectively to guide sperm to the spermatheca, the fertilization site (Fig. 1A) (7). The worm's transparent epidermis facilitates direct tracking of fluorescently labeled motile sperm. More than 90% of sperm target the spermatheca (Z3) successfully 1 hour after mating (Fig. 1B).

We previously found that mutations in the *daf-7* transforming growth factor- β (TGF- β) ligand cause sperm-targeting defects (8). *daf-7*, which is expressed in amphid single (ASI) sensory neurons (Fig. 1A), functions in a population density sensing mechanism (11–13). DAF-7 signals are transmitted through DAF-1 type I and DAF-4 type II receptors (Fig. 1C) (14). Mutations in *daf-7*, the *daf-1* and *daf-4* receptors, or downstream *daf-8*

¹Division of Reproductive Endocrinology and Infertility, Department of Obstetrics and Gynecology, University of Alabama at Birmingham, Birmingham, AL 35294, USA. ²Department of Cell, Developmental and Integrative Biology, University of Alabama at Birmingham, Birmingham, AL 35294, USA. ³Department of Pharmacology and Toxicology, University of Alabama at Birmingham, Birmingham, AL 35294, USA. ⁴Department of Pediatrics, Vanderbilt University, Nashville, TN 37232, USA. ⁵Department of Chemistry, Louisiana State University, Baton Rouge, LA 70803, USA. ⁶Department of Cell and Developmental Biology, Vanderbilt University, Nashville, TN 37232, USA.

*Corresponding author. E-mail: mamiller@uab.edu

Late Pleistocene Human Skeleton and mtDNA Link Paleoamericans and Modern Native Americans

James C. Chatters, Douglas J. Kennett, Yemane Asmerom, Brian M. Kemp, Victor Polyak, Alberto Nava Blank, Patricia A. Beddows, Eduard Reinhardt, Joaquin Arroyo-Cabral, Deborah A. Bolnick, Ripan S. Malhi, Brendan J. Culleton, Pilar Luna Erreguerena, Dominique Rissolo, Shanti Morell-Hart and Thomas W. Stafford Jr.

Science **344** (6185), 750-754.
DOI: 10.1126/science.1252619

American Beauty

Modern Native American ancestry traces back to an East Asian migration across Beringia. However, some Native American skeletons from the late Pleistocene show phenotypic characteristics more similar to other, more geographically distant, human populations. **Chatters *et al.*** (p. 750) describe a skeleton with a Paleoamerican phenotype from the eastern Yucatan, dating to approximately 12 to 13 thousand years ago, with a relatively common extant Native American mitochondrial DNA haplotype. The Paleoamerican phenotype may thus have evolved independently among Native American populations.

ARTICLE TOOLS

<http://science.sciencemag.org/content/344/6185/750>

SUPPLEMENTARY MATERIALS

<http://science.sciencemag.org/content/suppl/2014/05/14/344.6185.750.DC1>

RELATED CONTENT

<http://science.sciencemag.org/content/sci/344/6185/680.full>
<http://science.sciencemag.org/content/sci/347/6224/835.1.full>
<http://science.sciencemag.org/content/sci/347/6224/835.2.full>

REFERENCES

This article cites 70 articles, 7 of which you can access for free
<http://science.sciencemag.org/content/344/6185/750#BIBL>

PERMISSIONS

<http://www.sciencemag.org/help/reprints-and-permissions>

Use of this article is subject to the [Terms of Service](#)